

Order and Fluctuations in Nonequilibrium Molecular Dynamics Simulations of Two-Dimensional Fluids

M. Mareschal¹ and E. Kestemont¹

Received April 24, 1987

Finite systems of hard disks placed in a temperature gradient and in an external constant field have been studied, simulating a fluid heated from below. We used the methods of nonequilibrium molecular dynamics. The goal was to observe the onset of convection in the fluid. Systems of more than 5000 particles have been considered and the choice of parameters has been made in order to have a Rayleigh number larger than the critical one calculated from the hydrodynamic equations. The appearance of rolls and the large fluctuations in the velocity field are the main features of these simulations.

KEY WORDS: Molecular dynamics; hydrodynamic instability; fluctuations; nonequilibrium correlations.

1. INTRODUCTION

Interest in dissipative structures⁽¹⁾ has been increasing in recent years. The theory, initially developed for physicochemical systems, has also found applications in biological and even social problems.⁽²⁾ Many of the ideas in nonequilibrium thermodynamics originated from earlier work on hydrodynamical instabilities and in particular the Bénard problem (e.g., Ref. 1, footnote to p. 159): when a fluid layer is heated from below, at some critical value of the imposed temperature gradient convection starts and the heat is transported across the fluid by a mass flow that is structured in space. This is referred to as the Rayleigh–Bénard instability, a phenomenon extensively studied since the early experiments by Bénard and the theoretical interpretation given by Rayleigh.⁽³⁾ The transition to convection

¹ Faculté des Sciences, Université Libre de Bruxelles, B 1050 Bruxelles, Belgium.

has attracted much interest because it is a relatively simple situation in which to study the microscopic mechanisms involved in the onset of a dissipative structure.

Whereas the importance of fluctuations in nonequilibrium has often been stressed,⁽⁴⁾ a truly microscopic theory is far from complete. Results obtained from kinetic theory⁽⁵⁾ are limited to dilute gases. Fluctuating hydrodynamics has been used as an alternative⁽⁶⁻⁸⁾ to characterize the fluctuations that grow when approaching the instability. The experimental confirmation of these theories has not yet been obtained, as it seems that the observation would be limited to situations very close to the instability point⁽⁹⁾ and hence difficult to observe.

Numerical simulations have been intensively used to investigate non-equilibrium states.^{(10,11),2} Surprisingly, systems made of a few hundred to a few thousand particles appear to reproduce macroscopic behavior. Molecular dynamics (MD) experiments have led us to study the properties of fluids maintained very far from equilibrium.⁽¹²⁾ In particular, we have shown that, even under the extreme constraints that have to be imposed on the simulated fluids to obtain sufficient signal-to-noise ratios, these properties could be described very well by first-order corrections to local equilibrium distributions.³ The direct simulation methods have been applied to the study of long-range correlations that are present in non-equilibrium systems: for instance, the temperature fluctuations of a fluid in a temperature gradient are correlated all over the system size so that the fluid behaves in a very coherent way; the effects that are measured are small, but these experiments have permitted confirmation of theoretical predictions.^(14,15)

The simulation of the transition to rolls in heated fluids in the presence of an external field had not been done, as it was generally believed that the number of particles, as well as the times of integration, were too demanding from a computational point of view. The Rayleigh number is proportional to the third power of the layer thickness. As the largest systems simulated by molecular dynamics are at most equivalent to samples of the order of 1000 Å in size, one has to increase greatly the constraints to reach values near the critical ones. In our experiments, the temperature gradient expressed in usual units is as high as 100 million K/cm and the acceleration due to the external field is nearly 10^{11} cm/sec² (see Table I). Even if these values are obviously not comparable with those of a true laboratory experiment, model fluids placed in these situations seem to

² Also see the special issue on nonequilibrium fluids in *Physics Today* (January 1984).

³ This is truer for thermal than for velocity constraints, as many studies on non-Newtonian flows have shown (e.g., Ref. 13).

obey the simple macroscopic laws (see Refs. 11–13), and indeed this can be understood, as the change in the macroscopic averages remains small over distances of a mean free path. This led us to believe in the feasibility of a simulation of an atomic fluid showing the onset of convection and to finding an answer to the question of the minimum number of atoms involved in such a MD convection “experiment.”

In this article we report the first results obtained. The macroscopic description of the fluid in the range of parameters chosen would show convective transport of heat, and the transition to the roll structure. It turns out that the instability occurs even with a very small number of particles (less than 10,000). Besides, the fluctuations that we observe in the velocity field are very important. The results we present here open the way, in our opinion, to a new method of investigation of these questions.

The article is organized as follows: in the next section, we present the model and its properties. Then we describe the simulations done and give some of the measured quantities. We then discuss the results and end with an outline of the limitations and perspectives of the method, from both physical and computational viewpoints.

2. THE MODEL

The system is made up of 5040 hard disks placed in a rectangle of sides L_x and L_z with $L_x/L_z = 2 \cdot \sqrt{2}$; the z axis is chosen parallel to the vertical direction. A temperature difference ΔT is maintained between the two horizontal boundaries using a mechanism described below. A constant external force acts on the particles, corresponding to a gravitational acceleration g pointing in the $-z$ direction. The units we use are such that the disk diameter is 1, as is the disk mass and the upper plate temperature. In these units, we have set ΔT to 9, and g is *a priori* derived from the equality $mgL_z = k_B \Delta T$, where k_B is Boltzmann’s constant, expressing the fact that the average increase of kinetic energy of a particle at the hot boundary is sufficient to bring it to the top of the system. To discuss the choice of the geometrical and force parameters used, we first look at the dependence of the Rayleigh number (Ra) characterizing the state of a two-dimensional hard-disk fluid heated from below, as a function of density⁽³⁾

$$\text{Ra} = \alpha \Delta T g L_z^3 / \nu D_T \quad (1)$$

where $\alpha = (1/V)(\partial V/\partial T)_p$ is the thermal expansion coefficient, ν is the kinematic viscosity, and D_T is the thermal diffusivity. The values of the transport coefficients are obtained using the Enskog approximation at the temperature at $z = L_z/2$. Results are plotted in Fig. 1. As can be seen, the

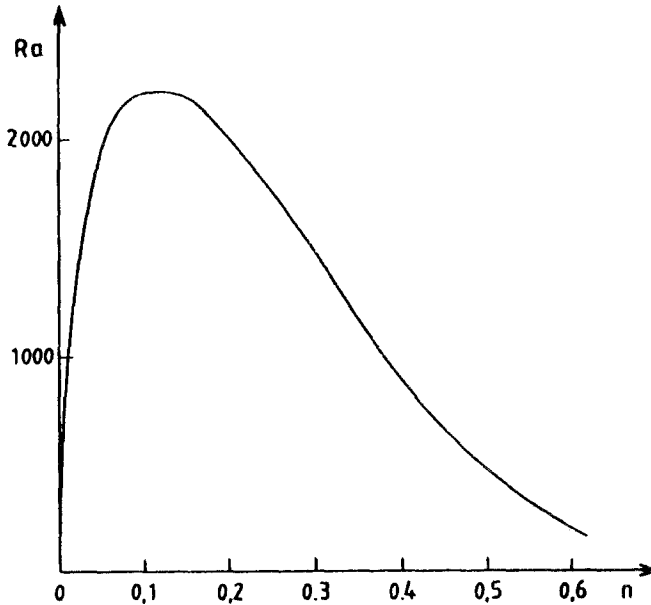


Fig. 1. Rayleigh number (Ra) computed for a hard-disk fluid of 5000 particles in a rectangular box with $L_x/L_z = 2 \cdot \sqrt{2}$. Temperature difference is 9, and the temperature at $L_z/2$ is taken to be 6. The Ra is proportional to $N^{3/2}$.

Rayleigh number has a maximum for a moderate density around 0.1. This is mainly due to the fact that the transport coefficients have a minimum around that value. On the other hand, very low density implies a low collision frequency. We finally chose the density to be 0.2: the collision frequency⁽¹⁶⁾ at a temperature of 6 is $\Gamma = 1.04N$ (N being the number of particles), so that the mean free path can be estimated to be 1.50. The thickness of the layer is 94.02, which is more than 60 mean free paths. The typical hydrodynamic time is usually taken to be the time necessary for heat to diffuse from bottom to top: here it corresponds to $(D_T/L_z^2)^{-1} \Gamma = 5 \cdot 10^6$ collisions.

Initially, the disks are placed uniformly in the rectangular box. The particles are given velocities depending on their positions and chosen from the corresponding local Maxwellian distribution, starting from a supposed linear temperature profile from the cold to the hot boundary. The evolution of the system is then followed in time. Particles move under the influence of the external field between collisions, which are instantaneous. Every time a disk hits one of the horizontal sides, it is first kept there for a while; it is then reinjected in the system with a velocity chosen from an equilibrium distribution function at the local wall temperature. The time of reintro-

Table I. Simulation Parameters^a

ΔT	g	$T(z = L_z/2)$	N_c	D_T	ν
4	0.05	3	17	6.77	2.98
5	0.06	3.9	13	7.72	3.4
5	0.07	3.9	12	7.72	3.4
9	0.09	6.2	35	9.74	4.28

^a Listed, respectively, are the reservoir temperature difference, the amplitude of the external force, the measured temperature at $z = L_z/2$, the number of collisions performed in the simulation (in millions), the values computed for the thermal diffusivity, and the kinematic viscosity.⁽¹⁶⁾ For all our runs, the ratio of the thermal energy to the energy of viscous dissipation of a roll is $k_B T/\nu^2 L_z n = 0.018$, as compared to 10^{-9} in typical laboratory experiments.

duction is such that the frequency is nearly constant and that incident fluctuations are absorbed at the boundary. This mechanism is probably not very important since, at most 3–4 particles are so “frozen” on a given wall. The sign of the tangential component of the velocity is conserved. This is in order to modify as little as possible the flow patterns. The vertical sides of the box are specularly reflecting walls: preliminary runs had indeed shown that periodic boundary conditions in the horizontal direction are not favorable to the onset of stable, long-lived structures.

All the parameters for the runs done are listed in Table I: in all cases the Rayleigh number is approximately 1800. If we convert to more usual units, and set the average temperature to be the room temperature, the atomic diameter to be 3 Å, and the thermal speed to be 1500 m/sec, the parameters of the last line of Table I refer to a simulation of a fluid experiencing a temperature gradient of $150 \cdot 10^6$ K/cm and an external acceleration of $6 \cdot 10^{11}$ cm/sec², and the total duration of the run lasts for $5 \cdot 10^{-9}$ sec.

3. THE SIMULATIONS

The system is divided into 20 by 50 cells. In each cell, one computes the time average of the velocity and of the number of particles. The time step is one-tenth of the unit time, i.e., one-fifth of the relaxation time. Figures 2–11 describe the velocity fields obtained as the average velocity times the mean number of particles in each cell, and their evolution in time. The corresponding arrows are normalized for each graph. In each MD experiment, the first 2 million of collision are not taken into account, as there is a violent transient taking place, with important variations of the

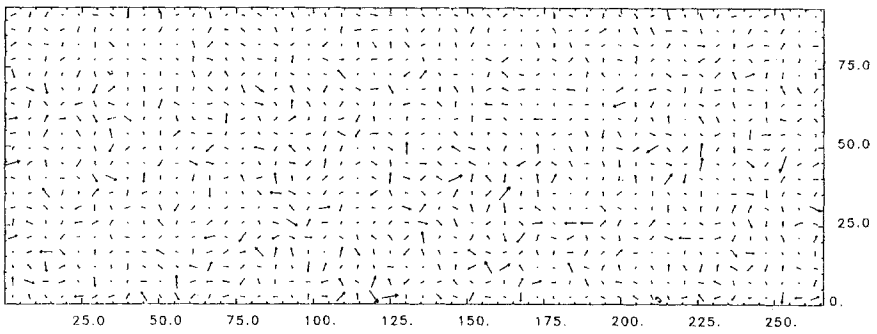


Fig. 2. Initial velocity field for $AT=9$ and $g=0.09$.

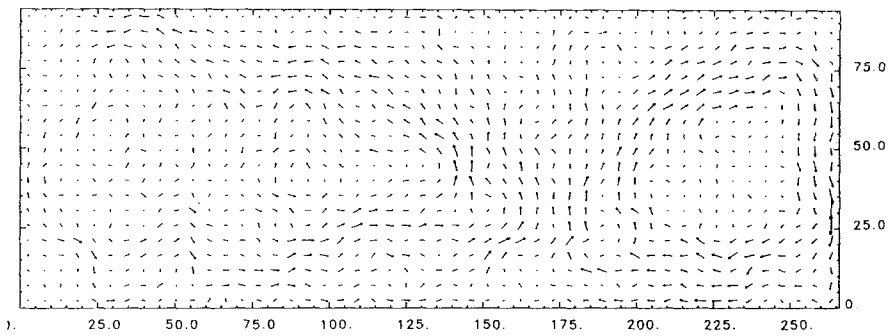


Fig. 3. Result corresponding to $t=340$ after the average has started ($N_c = 1.7 \cdot 10^6$).

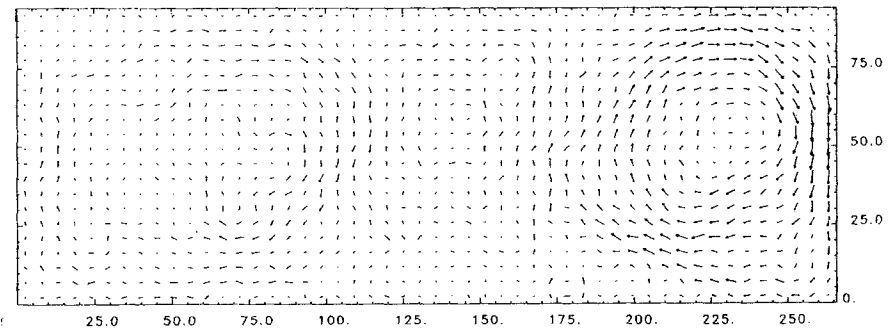


Fig. 4. Result for $t=430$ ($N_c = 2.2 \cdot 10^6$).

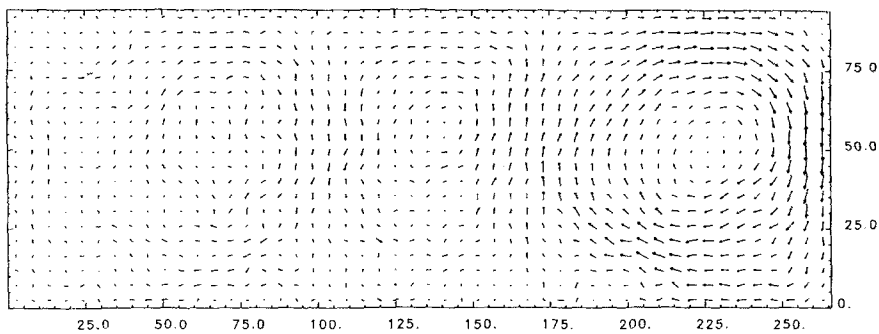


Fig. 5. Result for $t = 700$.

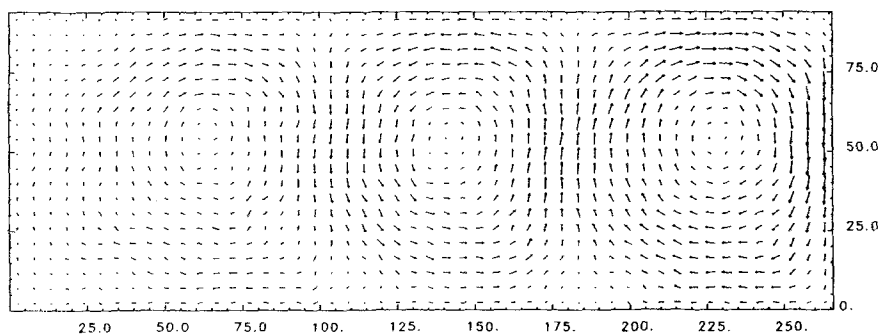


Fig. 6. Result for $t = 2720$.

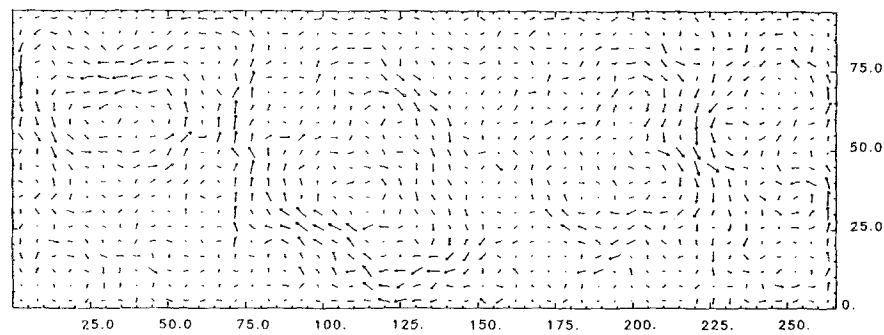


Fig. 7. Result for $t = 5400$, the time average extending only over the last 1900 time units.

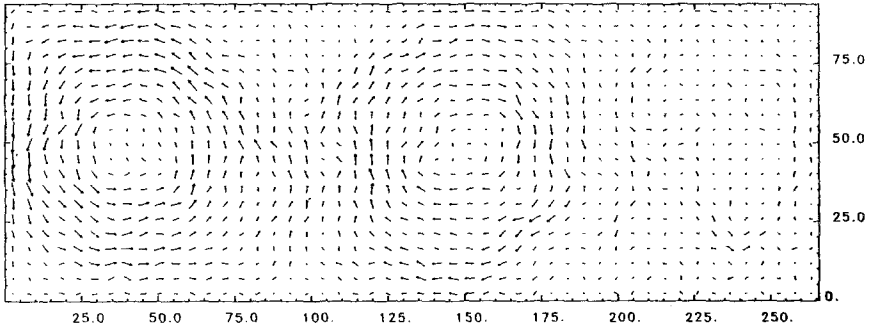


Fig. 8. Result for $t = 6400$, with a time average computed during the last 430 time units.

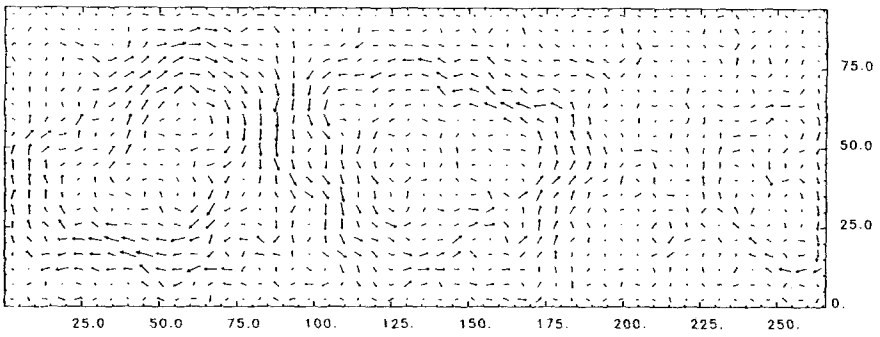


Fig. 9. Result for $\Delta T = 4$ and $g = 0.05$, $t = 430$.

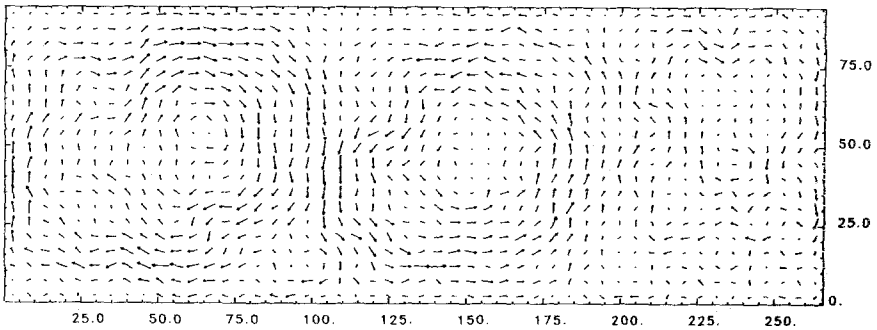


Fig. 10. Same as Fig. 8, for $t = 1080$.

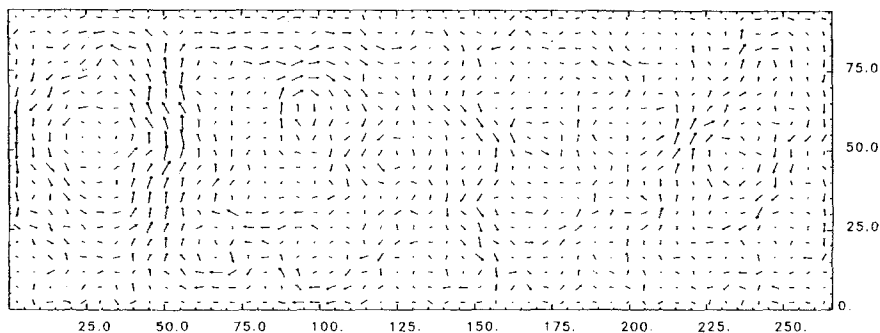


Fig. 11. Same as Fig. 9, for $t = 3030$.

total energy and momenta, through exchanges with thermal boundaries and between kinetic and potential energy during the initial evolution of the system toward a stationary state. Figures 2–7 correspond to a particular run at different times. In Fig. 3 we represent the velocity field for $t = 340$: this corresponds to 1.8 million collisions, or 700 collisions per particle. One already sees a vortex at the right of the box, with a flow going downward near the $x = L_x$ boundary. At $t = 430$, a second roll starts to form at the left of the first one. The highest cell velocities at that time correspond to a velocity per particle around 0.5; this is to be compared to the mean thermal velocities, ranging from 1.4 to 4.5. From $t = 700$ to $t = 2720$ the rolls become more and more regular and they extend progressively from the right to the left of the box. Approximately 5000 collisions per particle have taken place, for a total duration roughly equal to three diffusion times.

If we continue to follow the system in time, then, progressively, the structure fades out and other vortices are created as can be seen in Fig. 7. This is probably due to large fluctuations in the system near the thermal boundaries, which compete with the existing rolls. Figure 8 shows the appearance of a new structure with inverted flows. This occurs after a time interval roughly equal to the horizontal diffusion time.

In a series of other experiments, we decided to see what the effect of a change in the external parameters could be. Figures 9–11 give the velocity patterns observed for smaller values of the gravitational field and of the temperature gradient. In these new cases, one no longer has the same very well-defined convective cells, although spatial structure in the fluid remains partially present. It is to be noted that, in the first experiment as well as in the following ones, the Rayleigh number is still of the same order, i.e., 1800. We probably are very near the critical point, which could explain the long-time disappearance of the rolls in one experiment, and the difficulty of establishing a stable structure in the others.

The measurement of the mean number density is simple, although a question remains as to the minimum size required for the cell in which it is made; one has to keep in mind that we are dealing with “semimacroscopic” structures. To be able to see the flows, if present, we were obliged to chose a small enough cell size, which by no means is macroscopic. Until bigger systems become tractable by numerical simulation, it is not possible to make another choice. For the local temperatures, the difficulty is twofold. One is confronted with the problem of the small size of the cell and also of the fluctuations, over large time scales, of the local drift velocity. Indeed, the usual definition of temperature is given by the formula

$$k_B T_x^{(1)} = \left\langle 1/(N_x - 1) \sum_{i \in \alpha} m/2(\mathbf{v}_i - \mathbf{u}_\alpha)^2 \right\rangle \quad (2)$$

where α is the cell index, and $\langle \dots \rangle$ denotes a time average. The instantaneous cell velocity is

$$\mathbf{u}_\alpha = 1/N_\alpha \sum_{i \in \alpha} \mathbf{v}_i \quad (3)$$

with N_α the number of particles in the a cell, $N_\alpha = \sum_{i \in \alpha} 1$, and \mathbf{v}_i is the velocity of particle i . Results obtained using Eq. (2) are shown in Fig. 12b, where they are compared with a calculation of the local temperature using the equation of state

$$k_B T^{(2)} = p(1 - n\pi/4)^2/n[1 + (n\pi)^2/128] \quad (4)$$

This equation is known to correctly reproduce equilibrium simulation results in the range of density we are dealing with.⁽¹⁷⁾ In Eq. (4), the values for the pressure p and the number density n are obtained by measurements in 20 horizontal slices, each one containing on the average $N_s = 250$ particles. This large number of particles associated with the local measure of the pressure is important in the sense that the result is much less dependent on the existence of local currents. The pressure profile is shown in Fig. 12a together with the profiles of the local number density and kinetic energy of the particles given by

$$k_B T_s^{(3)} = \left\langle 1/N_s \sum_{i \in s} m v_i^2/2 \right\rangle \quad (5)$$

Equation (5) can also be used to measure the local temperature provided we correct it by subtracting the kinetic energy of the local flow, $m/2\langle u_s \rangle^2$. This correction, however, is of little effect and the difference between the three possible expressions for the temperature remains, essentially due to

the large fluctuations in the velocity field. The existence of such important fluctuations is confirmed by Figs. 9–11, where the velocity fields that develop in the absence of stable structured states are shown. From these figures, it is obvious that small whirlpools exist anyway in the system and they remain present for times of the order of the characteristic hydrodynamic time. These velocity fluctuations can also be directly

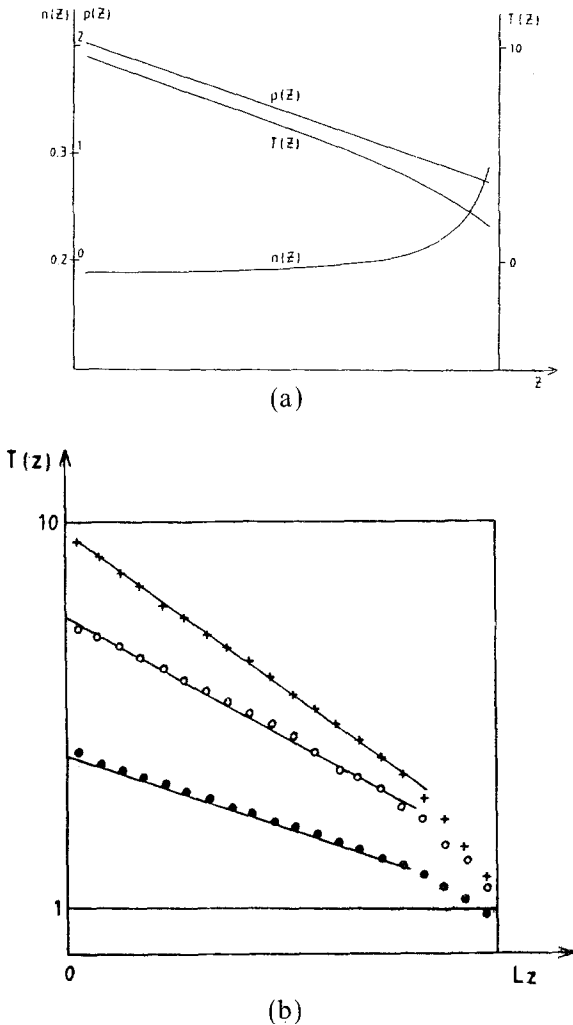


Fig. 12. (a) Number density, pressure, and temperature as functions of the z coordinate for the run where $\Delta T=9$ and $g=0.09$. (b) The temperatures obtained using Eqs. (5) (upper curve), (4), and (2) (lower curve), respectively.

measured: the mean square displacement [$\langle (nu)^2 \rangle - \langle nu \rangle^2$]^{1/2} is of the same order of magnitude as $\langle |nu| \rangle$.

The pressure profile is linear, even near the upper wall, where the boundary layer is more pronounced than near the lower plate. This is also shown by Fig. 13, where the measure of the local heat flux is given as a function of the altitude: the kinetic part of this heat flux is, as usual, given by

$$(J_{qz}^{\text{kin}})_\alpha = \left\langle \frac{1}{V_\alpha} \sum_{i \in \alpha} \frac{m}{2} (\mathbf{v}_i - \mathbf{u}_\alpha)^2 (v_{zi} - u_{z\alpha}) \right\rangle \quad (6)$$

whereas the potential part refers to energy transfer at collisions. This definition of the heat flux does not take into account energy transport associated with mass flux. The maximum in the heat flux which is observed near the boundaries is then interpreted as the impossibility for mass transport to take place in the z direction in the vicinity of the thermal plates.

This boundary layer has also some effect on the velocity distribution function: the moment ratio $\langle v^2 \rangle^2 / \langle v^4 \rangle$ measured as a function of z in the $\Delta T = 9$ run does not differ by more than 1% from its gaussian value (1/2) in the bulk. Near the lower plate it differs by 2% and near the upper boundary the difference is nearly 10%. In addition, it extends over one-fifth of the system thickness, which corresponds to the more pronounced variation of the number density (Fig. 12a).

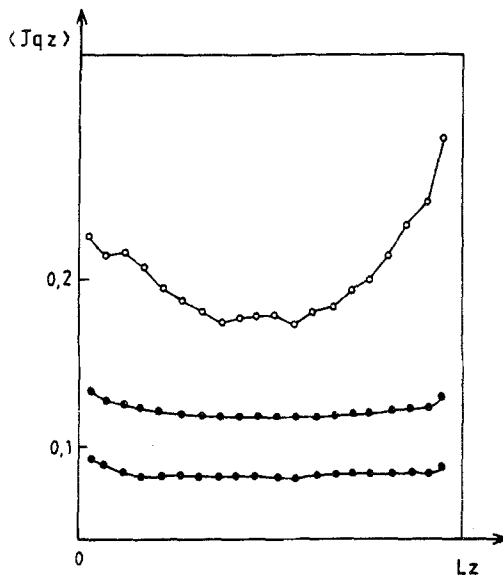


Fig. 13. Heat flux profiles for different gradients. The different ΔT are, respectively, 4, 5, and 9.

4. DISCUSSION

The results presented here confirm that the macroscopic hydrodynamic description already applies at distances of a few mean free paths and times of the order of the molecular characteristic times. Equilibrium simulations had already shown, e.g., that density fluctuations in a fluid of a few hundred particles could be understood on the basis of linear hydrodynamic equations. More recent work has shown that direct simulations of systems far from equilibrium could also be simulated by assemblies of a few hundred to a few thousand particles: it was, however, believed that a system size of at least 10^5 particles was necessary to simulate hydrodynamic instabilities. Not so! The first conclusion that we can draw from our simulations is that systems of 5000–10,000 particles are able to display the onset of convection in a fluid heated from below. This is important, as systems of that size can easily be studied on modern supercomputers. We are aware, however, that a more precise comparison has to be made with macroscopic results before MD can be safely used to model these phenomena. This is still in progress.

With respect to laboratory experiments or to macroscopic numerical simulations, molecular dynamics permits us to extend the domain of investigation. Indeed, fluctuations are not present in the macroscopic description and we know they play an important role in the approach to instability, but only in a narrow region near the critical point and yet unobservable in laboratory experiments. Of course, in MD, the magnitude of the constraints that have to be imposed on the fluid are orders of magnitude higher than realistic ones. However, we are still in a region where a simple linear relation between thermodynamic fluxes and forces is now known to hold, that is, these constraints can still be considered as perturbations with respect to a local equilibrium description. The picture that we gain of what happens on a microscopic scale near an instability is that of a competition between the thermal fluctuations and the velocity fluctuations, which tend to become structured. If the constraint is sufficiently large, the study of these phenomena is easier by molecular dynamics, because there the ratio of the thermal noise to the heat dissipated by the rolls is much larger than in true laboratory experiments.

Limitations in precision are due to the small size of the cells in which the measurements are done. Larger systems have to be considered. This is also the case if we want to reach higher values of the Rayleigh number, where turbulence sets in. The Ra is proportional to $N^{3/2}$ in our two-dimensional systems. If we want to keep a nearly constant density, we have to take into account the dependence we impose between the external field and the size of the system. This then gives us a Rayleigh number proportional

to N . For example, Rayleigh numbers of order 50,000 will require systems composed of about 10^5 particles. Such simulations may have to wait for a new generation of computers: although they are at present technically possible, they may be too costly with respect to computer time.

Recently, an interesting approach has been developed using the so-called "cellular automata" models. Simplifying as much as possible the underlying atomic dynamics, they have proved successful in displaying some turbulent behavior.⁽¹⁸⁾ The behavior of these models is much easier to follow and much faster and systems of several millions of particles can be studied. However, they have not yet proved useful for systems under thermal constraints. Still another approach, more interesting for temperature-dependent phenomena, is the direct simulation method of the Boltzmann equation.⁽¹⁹⁾ It is, however, limited to dilute gases where the Rayleigh numbers for the same N systems are much smaller. The extension of similar methods to the moderately dense fluids would make them competitive with MD.

ACKNOWLEDGMENTS

We are grateful to Prof. I. Prigogine for constant encouragement. We thank Prof. G. Nicolis and Drs. M. Malek Mansour and A. Garcia for stimulating discussions. The computation was done within the program financed by the Fonds National de la Recherche Scientifique in collaboration with IBM-Belgium. Financial assistance for one of us (M. M.) from the Actions de Recherches Concertées program is gratefully acknowledged.

REFERENCES

1. P. Glandsdorff and I. Prigogine, *Thermodynamic Theory of Structure, Stability and Fluctuations* (Wiley-Interscience, New York, 1971).
2. G. Nicolis and I. Prigogine, *Self-Organisation in Nonequilibrium Systems* (Wiley-Interscience, New York, 1977).
3. S. Chandrasekhar, *Hydrodynamic and Hydromagnetic Stability* (Clarendon Press, Oxford, 1961).
4. A. M. S. Tremblay, in *Recent Developments in Non-Equilibrium Thermodynamics*, J. M. Rubi, G. Lebon, and J. Casas-Vasquez, eds. (Springer, Berlin, 1984).
5. R. Smitz and E. G. D. Cohen, *J. Stat. Phys.* **40**:431 (1985).
6. J. Swift and P. C. Hohenberg, *Phys. Rev. A* **15**:319 (1977).
7. R. Graham, *Phys. Rev. A* **10**:1762 (1974).
8. V. M. Zaitsev and M. I. Schliomis, *Sov. Phys. JETP* **32**:866 (1977).
9. G. Ahlers, M. C. Cross, P. C. Hohenberg, and S. Safran, *J. Fluid Mech.* **110**:297 (1981).
10. D. J. Evans and W. G. Hoover, *Annu. Rev. Fluid Mech.* **18**:243 (1986).

11. G. Ciccotti and W. G. Hoover (eds.), *Molecular-Dynamics Simulation of Statistical-Mechanical Systems* (North-Holland, Amsterdam, 1987).
12. M. Mareschal, E. Kestemont, F. Baras, E. Clementi, and G. Nocolis, *Phys. Rev. A* (1987), to appear.
13. D. J. Evans, H. J. M. Hanley, and S. Hess, *Phys. Today* **26**, (January 1984).
14. M. Mareschal and E. Kestemont, *Phys. Rev. A* **30**:1158 (1984).
15. M. Malek Mansour, A. L. Garcia, G. C. Lic, and E. Clementi, *Phys. Rev. Lett.* **58**:874 (1987).
16. D. M. Gass, *J. Chem. Phys.* **54**:1898 (1971).
17. J. A. Barker and D. E. Henderson, *Rev. Mod. Phys.* **48**:587 (1976).
18. U. Frisch, B. Hasslacher, and Y. Pomeau, *Phys. Rev. Lett.* **56**:1505 (1986).
19. J. A. Bird, *Molecular Gas Dynamics* (Clarendon Press, Oxford, 1976).